ON-LINE APPENDIX

Data Acquisition

All imaging experiments were performed on a 3T MR imaging system with a maximum gradient strength of 45 mT/m and a maximum single-direction slew rate of 200 mT/m/ms (Tim Trio, Siemens) by using a twice-refocused balanced spin-echo diffusion echo-planer imaging pulse sequence[1] with fat suppression. Each session included independent DSI and DKI acquisitions, with the DTI data being taken as a subset of the DKI acquisition. Each volunteer was scanned during 2 separate sessions, resulting in 6 complete DSI and DKI datasets to quantify variability for each DWI method. The DWI protocols were optimized, to maximize the SNR rather than minimize the acquisition times, to facilitate the assessment of the accuracy of the DKI and DTI fiber-orientation estimates relative to those of DSI.

Acquisition parameters common to both DSI and DKI acquisitions were the following: voxel size = 2.7 × 2.7 × 2.7 mm^3, matrix = 82 × 82, number of sections = 45, bandwidth = 1356 Hz/pixel, and a 32-channel head coil with an acceleration factor of 2 by using generalized autocalibrating partially parallel acquisition[2] and adaptive combine coil mode.[3] Additional parameters for the DSI acquisition were TR/TE = 8300/151 ms and 515 diffusion-encoding gradient directions over a Cartesian grid with a maximum b-value of 6000 s/mm^2, which was optimized for diffusion sensitivity and gradient performance,[4] resulting in a total acquisition time of 71.7 minutes. For the DKI acquisitions, additional parameters were TR/TE = 6100/102 ms, 64 diffusion-encoding gradient directions at b-values of 1000 s/mm^2 and 2000 s/mm^2, and 20 independent acquisitions without diffusion-weighting (b0 images), resulting in a total acquisition time of 15.6 minutes. In both cases, the TE was minimized to maximize SNR. DTI data were also analyzed by using the 0 and 1000 s/mm^2 b-value images from the DKI dataset. During each session, an additional T1-weighted magnetization-prepared rapid acquisition of gradient echo image with 1.0 × 1.0 × 1.0 mm^3 voxel dimensions was also acquired for anatomic reference. If one assumes 80% of the maximum gradient strength (45 mT/m), ie, 36 mT/m, was used to achieve the minimum TE, δ and Δ can be estimated at 32 and 74 ms for the DSI scan and 22.5 and 50 ms for the DKI scan, respectively.

dODF Reconstructions

Each scan for each subject was coregistered to the subject's initial DSI scan by using a 12-parameter affine transformation with SPM12 (http://www.fil.ion.ucl.ac.uk/spm/software/spm12). Following coregistration, we applied spatial smoothing to all diffusion-weighted images to reduce the effects of signal noise by using a Gaussian smoothing kernel of 1.25 times the voxel dimensions.[5]

The intravoxel DSI dODF was reconstructed by using DSI Studio (dsi-studio.labsolver.org) with a Hanning filter, width 17, applied to the *q*-space data. DKI-derived diffusion and kurtosis tensors were calculated by using a constrained weighted linear least squares algorithm,[5] and the DKI dODF was calculated by using the closed-form solution derived by Jensen et al.[6] The DTI-derived diffusion tensor was obtained by using weighted linear least squares.[7] Following previous studies, the radial weighting power was set to $\alpha = 2$ for DSI[8,9] and $\alpha = 4$ for DKI.[6,10,11] For visualization of DTI dODFs, the radial weighting power was set to $\alpha = 4$; however, this had no effect on the DTI-derived orientation estimates.[6,10] All orientations were corrected for rotations of the image volume that occurred during image acquisition and coregistration.[12] The kurtosis dODF reconstruction was performed by using the Diffusional Kurtosis Estimator Fiber Tractography Module (https://www.nitrc.org/projects/dke/), and the DTI dODF was reconstructed by using in-house software.

Data Analysis

Angular variability of the dODFs was calculated by the absolute voxelwise angular difference for each reconstruction between the principal orientation (the orientation corresponding to the global maxima pair) from the first scan and the nearest orientation from the second scan. Angular errors in the DKI and DTI dODFs were calculated by using the absolute angular differences between the principal orientation from the corresponding DSI scan and the nearest dODF maximum from the respective reconstruction. For angular difference measures, the nearest orientation in the second scan was chosen as opposed to the global maximum from the second scan because small fluctuations in dODF magnitudes in voxels with multiple orientation estimates could vary which orientation was identified as the global maximum, resulting in artificially large angular differences.[10] Angular error estimates include intrinsic variability in the reconstruction techniques and hence combine both random and systematic error. In addition, because absolute differences are used, these measures are positively biased by noise and will consequently overestimate the true systematic differences.

To quantify angular variability and angular error, we defined ROIs for each subject. These included an inclusive WM ROI, which was defined as voxels with FA > 0.1; a conservative WM ROI, which was defined as voxels with FA > 0.3; a single-fiber-bundle ROI, which was defined as voxels within the inclusive WM ROI with the estimated number of fiber directions = 1 in the DSI scan; 2 crossing-fibers ROI, which was defined as voxels within the inclusive WM ROI with the number of fiber directions = 2 in the DSI scan; and a ≥3 crossing-fibers ROI, which was defined as voxels within the inclusive WM ROI with the number of fiber directions ≥ 3 in the DSI scan. To reduce CSF partial volume effects, we excluded voxels within each ROI with a mean diffusivity of >1.5 μm^2/ms from quantitative analyses.[6,10] To help reduce the occurrence of spurious peaks in the DSI reconstruction, we used a quantitative anisotropy threshold of 0.1 to filter the DSI orientations.[13]

To visualize group differences in the angular variability and angular error measures, we normalized parameter maps from each subject to the International Consortium for Brain Mapping WM template[14] by using SPM12 with nonlinear registration, and we constructed average, group-wise parameter maps.

Tractography

WM fiber tractography was performed with DSI Studio by using the Euler method[15] with a step size of 1.35 mm, a minimum track length of 20 mm, and a maximum track length of 450 mm. For direct and qualitative comparisons across the 3 techniques, we defined a common WM tracking ROI to include

regions in the inclusive WM ROI with quantitative anisotropy of >0.1 in the DSI scan. The fiber-tracking algorithm was seeded with 200,000 random seed points within the WM tracking ROI. WM fiber tracts were visualized by using TrackVis (http://www.trackvis.org).

REFERENCES

1. Reese TG, Heid O, Weisskoff RM, et al. **Reduction of eddy-current-induced distortion in diffusion MRI using a twice-refocused spin echo.** *Magn Reson Med* 2003;49:177–82 CrossRef Medline
2. Griswold MA, Jakob PM, Heidemann RM, et al. **Generalized autocalibrating partially parallel acquisitions (GRAPPA).** *Magn Reson Med* 2002;47:1202–10 CrossRef Medline
3. Walsh DO, Gmitro AF, Marcellin MW. **Adaptive reconstruction of phased array MR imagery.** *Magn Reson Med* 2000;43:682–90 Medline
4. Kuo LW, Chen JH, Wedeen VJ, et al. **Optimization of diffusion spectrum imaging and q-ball imaging on clinical MRI system.** *Neuroimage* 2008;41:7–18 CrossRef Medline
5. Tabesh A, Jensen JH, Ardekani BA, et al. **Estimation of tensors and tensor-derived measures in diffusional kurtosis imaging.** *Magn Reson Med* 2011;65:823–36 CrossRef Medline
6. Jensen JH, Helpern JA, Tabesh A. **Leading non-Gaussian corrections for diffusion orientation distribution function.** *NMR Biomed* 2014; 27:202–11 CrossRef Medline
7. Basser PJ, Mattiello J, Le Bihan D. **Estimation of the effective self-diffusion tensor from the NMR spin echo.** *J Magn Reson* 1994;103: 247–54 CrossRef Medline
8. Wedeen VJ, Hagmann P, Tseng WY, et al. **Mapping complex tissue architecture with diffusion spectrum magnetic resonance imaging.** *Magn Reson Med* 2005;54:1377–86 CrossRef Medline
9. Wedeen VJ, Wang RP, Schmahmann JD, et al. **Diffusion spectrum magnetic resonance imaging (DSI) tractography of crossing fibers.** *Neuroimage* 2008;41:1267–77 CrossRef Medline
10. Glenn GR, Helpern JA, Tabesh A, et al. **Optimization of white matter fiber tractography with diffusional kurtosis imaging.** *NMR Biomed* 2015;28:1245–56 CrossRef Medline
11. Neto Henriques R, Correia MM, Nunes RG, et al. **Exploring the 3D geometry of the diffusion kurtosis tensor: impact on the development of robust tractography procedures and novel biomarkers.** *Neuroimage* 2015;111:85–99 CrossRef Medline
12. Leemans A, Jones DK. **The B-matrix must be rotated when correcting for subject motion in DTI data.** *Magn Reson Med* 2009;61: 1336–49 CrossRef Medline
13. Yeh FC, Verstynen TD, Wang Y, et al. **Deterministic diffusion fiber tracking improved by quantitative anisotropy.** *PLoS One* 2013;8: e80713 CrossRef Medline
14. Mori S, Wakana S, Nagae-Poetscher LM, et al. *MRI Atlas of Human White Matter*. Amsterdam: Elsevier; 2005
15. Basser PJ, Pajevic S, Pierpaoli C, et al. **In vivo fiber tractography using DT-MRI data**. *Magn Reson Med* 2000;44:625–32 Medline

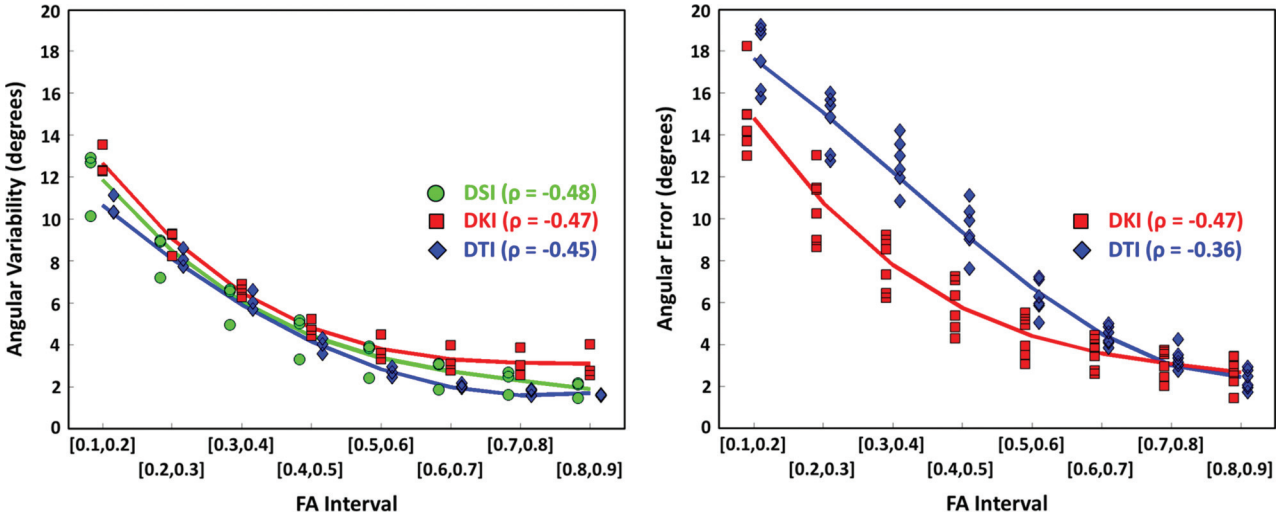

ON-LINE FIG 1. The performance of dODF-derived orientation estimates depends on FA, with angular variability and angular error decreasing with increasing FA. Data points for each group are averaged over the indicated interval and are separated in the horizontal direction within each interval for legibility. The Spearman rank correlation coefficient for the voxelwise performance measure relative to FA is indicated by ρ.

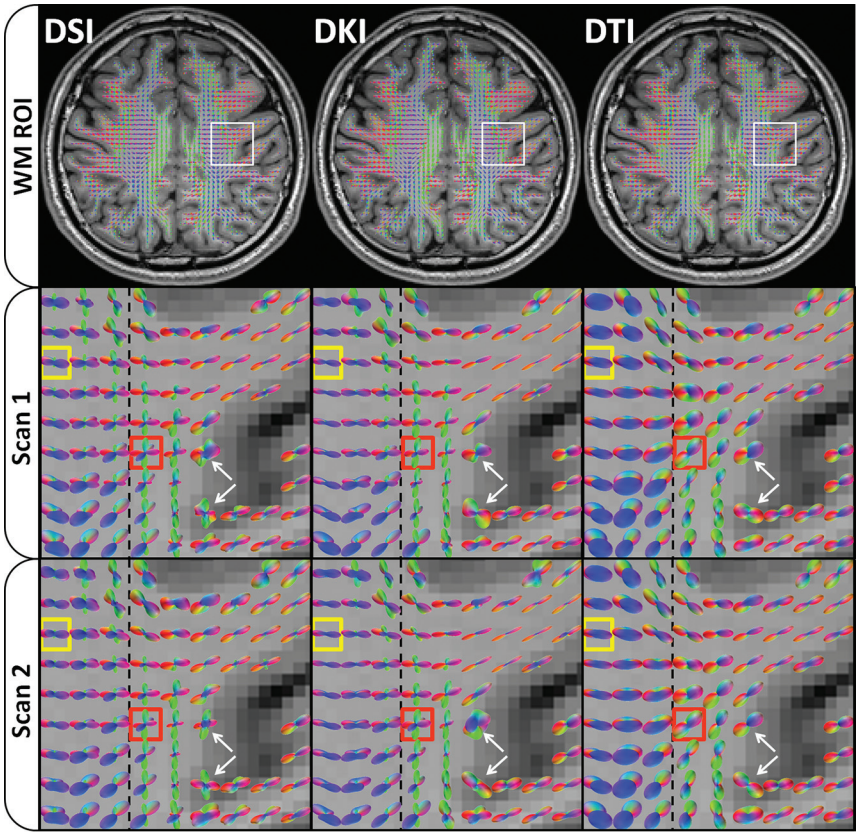

ON-LINE FIG 2. For each reconstruction, dODFs within the inclusive WM ROI are overlaid on the MPRAGE image for anatomic reference. The dODF reconstructions are qualitatively consistent between repeat scans, but DTI cannot detect crossing fibers (*red box*); this feature may increase angular error relative to DSI. DSI is more sensitive than DKI at detecting crossing fibers (*yellow box*). The inclusive WM ROI may include partial volume effects (*white arrows*), which may increase variability and error in orientation estimates.

On-line Table: dODF performance statistics in the FA- and NFD-defined WM ROIs[a]

		Angular Variability			Angular Error		Systematic Error[b]	
	No.	DSI	DKI	DTI	DKI	DTI	DKI	DTI
Inclusive WM ROI (FA > 0.1)								
Subject 1	33303	8.7 (9.7)	8.2 (9.4)	7.6 (9.9)	9.9 (10.4)	13.7 (13.8)	1.7	6.1
Subject 2	34087	9.5 (9.7)	9.9 (9.9)	7.7 (9.7)	11.4 (12.3)	14.0 (14.0)	1.4	6.3
Subject 3	35340	6.4 (7.6)	8.3 (9.3)	7.4 (9.3)	10.0 (10.4)	13.8 (14.1)	1.7	6.5
Mean	34243	8.2 (9.0)	8.8 (9.5)	7.6 (9.7)	10.4 (11.0)	13.8 (14.0)	1.6	6.3
Conservative WM ROI (FA > 0.3)								
Subject 1	13692	5.3 (5.7)	4.8 (5.6)	4.4 (5.8)	6.2 (6.6)	10.1 (10.7)	1.4	5.7
Subject 2	11418	5.4 (5.4)	5.8 (5.4)	4.3 (5.6)	6.2 (7.1)	9.4 (10.1)	0.4	5.2
Subject 3	16144	3.7 (4.6)	5.2 (5.7)	4.8 (6.3)	6.3 (6.9)	9.9 (10.7)	1.1	5.0
Mean	13751	4.8 (5.2)	5.3 (5.6)	4.5 (5.9)	6.2 (6.9)	9.8 (10.5)	1.0	5.3
Single-fiber ROI (NFD = 1)								
Subject 1	18808	8.3 (8.3)	7.8 (8.2)	6.4 (7.6)	9.0 (8.7)	10.2 (9.7)	1.2	3.8
Subject 2	18814	8.8 (8.2)	9.2 (8.4)	6.0 (6.4)	10.0 (9.9)	10.5 (9.7)	0.9	4.6
Subject 3	23573	6.3 (7.0)	8.0 (8.4)	6.2 (7.4)	9.4 (9.2)	10.9 (10.8)	1.4	4.7
Mean	20398	7.8 (7.8)	8.3 (8.4)	6.2 (7.1)	9.5 (9.3)	10.6 (10.1)	1.2	4.4
Two crossing-fiber ROIs (NFD = 2)								
Subject 1	11258	9.2 (10.9)	8.7 (10.3)	8.8 (11.5)	10.7 (11.7)	17.4 (16.2)	2.0	8.6
Subject 2	11404	10.0 (10.9)	10.5 (10.8)	9.3 (11.5)	12.4 (13.7)	17.4 (16.2)	1.9	8.1
Subject 3	9824	6.6 (8.6)	8.6 (10.4)	9.2 (11.6)	10.8 (11.8)	18.2 (16.7)	2.2	9.0
Mean	10829	8.6 (10.1)	9.3 (10.5)	9.1 (11.5)	11.3 (12.4)	17.7 (16.4)	2.1	8.6
Three or more crossing fibers (NFD ≥ 3)								
Subject 1	3237	9.7 (12.3)	9.0 (11.7)	10.4 (14.1)	12.6 (14.1)	22.4 (18.9)	3.5	12.0
Subject 2	3869	11.3 (12.4)	12.0 (13.1)	11.4 (14.5)	14.9 (16.6)	21.7 (19.4)	2.9	10.3
Subject 3	1943	7.7 (10.0)	10.1 (12.3)	11.6 (14.0)	13.2 (14.3)	24.8 (19.8)	3.0	13.2
Mean	3016	9.6 (11.6)	10.4 (12.4)	11.1 (14.2)	13.5 (15.0)	23.0 (19.4)	3.2	11.8

Note:—NFD indicates number of fiber directions as determined with DSI.

[a] The number of voxels in each ROI is indicated by "No.," and values for angular variability and angular error represent the mean (± SD) of the voxelwise performance measures throughout the ROI. All values are given in degrees.

[b] Defined as the difference between the mean angular error and the mean angular variability over each ROI for the respective reconstructions.